X-ray-photoelectron-spectroscopy and Auger-electron-spectroscopy study of ultrathin palladium films on a Pt(111) substrate

Moonsup Han, P. Mrozek, and A. Wieckowski
Department of Chemistry, University of Illinois, 600 South Mathew Street, Urbana, Illinois 61801
(Received 24 February 1993)

We have studied ultrathin palladium films vacuum deposited onto a Pt(111) substrate utilizing Auger-electron spectroscopy (AES), low-energy electron diffraction, and x-ray photoelectron spectroscopy. The AES results fit well to a layer-by-layer growth deposition. Below a coverage of 4 monolayers, the electron-diffraction data only show a (1×1) structure of palladium adatoms on the Pt(111) substrate, supporting the Frank–van der Merve growth mechanism. In contrast to two-dimensional palladium clusters and palladium bimetallic systems, the Pd 3*d* core-level binding energy of palladium on Pt(111) shifts toward lower binding energy relative to the value of bulk palladium with decreasing palladium overlayer coverage. This negative binding-energy shift of a surface adatom core level results mainly from the initial-state band-narrowing effect predicted by Citrin, Wertheim, and Baer. Also, the absence of the final-state effect after creating a core hole in the Pd/Pt(111) system indicates that efficient screening or very fast relaxation occurs, and that hybridization of the valence bands of the palladium adlayer and the platinum substrate plays an implortant role in the negative surface-atom binding-energy shift of the Pd 3*d* core level.

I. INTRODUCTION

Surface properties of ultrathin metal films deposited on foreign metal substrates are usually quite different from those of bulk substrate and deposit materials.[1–3] Therefore, various admetal-substrate metal composites have been investigated in the search for new effective catalysts and corrosion protective option.[1,2] Palladium—as a deposited material—has attracted considerable research interest because of the prospects for catalysis enhancement[4] and the potential for advancing our understanding of vacuum deposition processes *per se*.[1] For instance, submonolayer palladium films alter the electronic structure of chemisorbed carbon monoxide, as referenced to its properties on the surfaces of solid palladium.[5–10] This promises a new catalytic reactivity of such films toward organic compounds.

The deposition of palladium on the Pt(111) surface has also been carried out in electrolytic solutions.[11,12] The morphology and position of two narrow voltammetric peaks at 0.22 and 0.45 V (vs reversible hydrogen electrode), assigned to hydrogen adsorption/desorption, reflect electrode mechanisms that are not yet understood. Neither are the surface sites engaged in hydrogen adsorption nor the hydrogen surface coordinations known. These uncertainties must be cleared using a molecular-level approach. We begin to seek answers to the origin of the voltammetry and the electrode properties of the palladium films by studying *vacuum* prepared palladium deposits on the Pt(111) substrate. We believe that the results presented below will be transferable to electrochemical situations, which we are investigating in parallel.

Data on the electronic states and structures involved in formation of the Pd/Pt(111) interface by x-ray photoelectron spectroscopy (XPS) have not previously been reported. Studies with Pt(110) by field ion microscopy provided information on palladium adatom diffusion and on the thermal stability of the (1×1) palladium overlayers.[13] Palladium growth has also been investigated on several other noble-metal single-crystal substrates: Au(111),[10,14] Ag(111), and Ag(100).[15] Likewise, thin films of palladium-platinum alloys on a quartz substrate have been studied using Auger-electron spectroscopy.[16] On the other hand, excessive effort has been devoted to investigations of palladium clusters deposited on inert carbon substrates.[17–24] The main objective of the cluster studies was to understand the size-dependent electronic structure of the supported metal clusters for application in catalysis and to follow the transitions of electronic states from the isolated atoms to the bulk metal.[17–24] The origin of the binding-energy shift of the Pd 3*d* core level was studied in Refs. 3, 17, and 18. The core-level binding-energy shift was attributed to an initial-state band narrowing of surface atoms[3,25,26] and/or the final-state relaxation effect after creating a photoelectron.[3,17,18]

Since surface atoms have fewer neighbors than bulk atoms, the surface valence-band width which reflects the degree to which electrons are delocalized, should be narrower than the valence-band width of the bulk phase. Figure 1 shows schematically the band-narrowing effect on the surface-atom valence band. That is, the hybridized valence bands of nd and $(n+1)s$ ($n=3$, 4, and 5) are considered under the assumption of a constant density of states. Since the electronic charge tends to maintain neutrality even at the surface, i.e., same number of occupied electronic states per atom, the valence-band centroid shifts toward the Fermi level as the bandwidth narrows. As a consequence of the initial-state valence-band narrowing, a negative core-level binding-energy shift of the surface adatom is predicted for metallic elements with the valence band more than half filled as shown in Fig. 1(a).[25,26]

The negative binding-energy shift of the surface-atom core level with respect to the bulk value due to the initial-state band narrowing has been confirmed for pure elemental metals such as palladium and some other noble metals.[27,28] To distinguish between the spectral weight contributions to the core-level spectra from the surface and the bulk atoms, angle-dependent x-ray photoelectron spectra[27] or high-resolution photoemission spectra excited by synchrotron radiation[28] has been used. The similar negative core-level binding-energy shifts of the adatom have previously been seen for other bimetallic systems such as Cu/Rh(100), Cu/Ru(0001), Ni/Ru(0001),[30] and Au/Pt(100).[33] This shift has been interpreted as originating from the changes in the initial states caused by the variations in the coordination number,[25,33] and has been used to understand the properties of CO chemisorbed on bimetallic systems.[30]

On the other hand, the photoexcited final state of samples in the XPS is not always fully relaxed to the ground state of the $N-1$ system after a creating core hole. Although there are several definitions of the final-state effect, we define the final-state contribution to the core-level binding-energy shift as the total energy of the final state referenced to the fully relaxed ground state of the photoexcited $N-1$ system.[3] It has been found that many palladium clusters on various substrates and bimetallic systems display a core-level binding-energy (BE) shift toward higher BE compared to the bulk value.[17–23,29–32] Such a shift of the band-narrowed surface atoms has been shown for small palladium clusters,[17–23] palladium thin-film bimetallic systems,[29,30] and binary alloys.[31,32] This was mainly explained as a result of poor screening of the photoexcited core hole in the final state.[3,17,18]

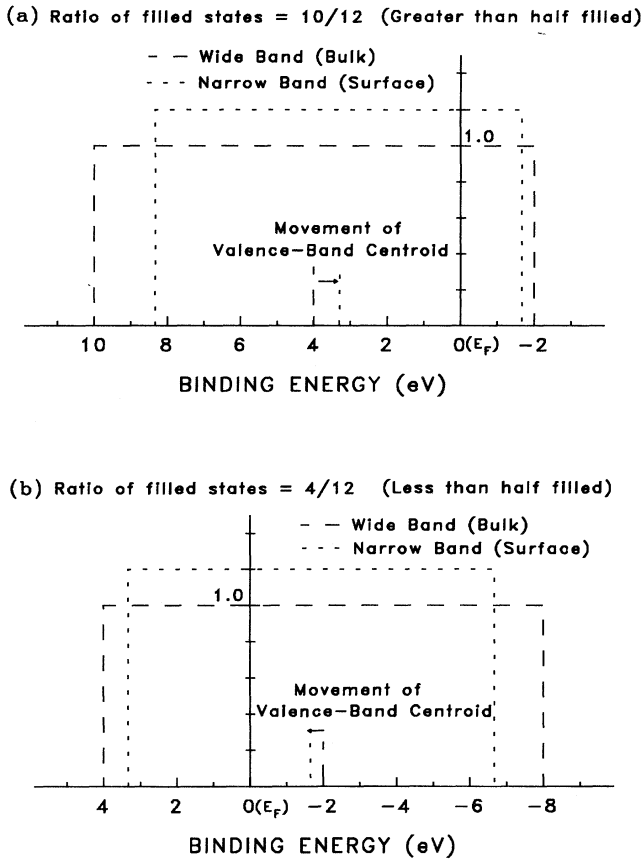

FIG. 1. Schematic explanation of the band-narrowing effect. The centroid of the narrowed surface-atom valence band shifts toward the Fermi level, i.e., (a) to the lower binding energy in the greater than half filled case and (b) to the higher binding energy in the less than half filled case.

In this work, we aim at obtaining an insight into the electronic and chemical properties of ultrathin palladium films vacuum-evaporated on the Pt(111) substrate. We have focused on the core-level binding-energy shift as a function of palladium coverage. With decreasing coverage, the palladium core-level binding energy shifts toward the lower binding energy, as compared to the bulk value. This result is in a clear contrast to the binding-energy data obtained with palladium clusters deposited on inert substrates,[17–23] as well as with the earlier mentioned bimetallic systems.[29–32] We note that the sign and amount of the core-level binding-energy shift are closely related to the width and the occupation of the valence band, and to the excited states of the deposit/substrate configurations.[30] We discuss the meaning of the negative binding-energy shift of the Pd $3d$ core level in detail. Because of our parallel electrochemical focus,[34] we believe that this study is a promising beginning of a combined understanding of ultrathin palladium deposits in electrochemistry and surface science.

II. EXPERIMENT

A disk-shaped platinum single crystal with a diameter of about 8 mm was polished and oriented in the (111) crystallographic plane to within 1°, as determined by Laue x-ray diffraction. Palladium was deposited on the Pt(111) crystal at room temperature by an evaporator made by wrapping 0.1-mm palladium wire around a 0.25-mm tungsten wire, and placed about 25 cm from the sample for uniform deposition. Heating the tungsten wire with 20 W resulted in a palladium deposition rate of about 1 ML/min. Between the dopings, the palladium source was kept hot but below the sublimination temperature, to secure a clean deposit. The base pressure of the UHV system was maintained at less than 3×10^{-10} torr. We cleaned the sample surface by repeatedly sputtering and annealing. Crystal structure and surface cleanliness were verified by low-energy electron diffraction (LEED) and Auger-electron spectroscopy (AES). The cleaning was done to the point where the amount of carbon determined by AES was less than 0.03 ML, and a clear hexagonal (111) crystal-face low-energy-electron diffraction pattern was shown. The x-ray photoelectron spectra were recorded with the Surface Science Instruments M-Probe ESCA system with the high-resolution spherical capacitor analyzer under fixed analyzer transmission (constant pass energy) mode. The source was a monochromatic Al $K\alpha$ line with 150-W power and was focused on an area with a 1-mm-diam spot size. The pass energy was 100 eV for the shallow core level (or valence band) and Pt $4f$ spectra, and 150 eV for the Pd $3d$ and Pt $4d_{3/2}$

spectra. Since metals usually show a very sharp drop in the number of occupied states at the Fermi level, the binding energies were calibrated by referencing the valence-band spectra to a step function at the Fermi level convoluted by a Gaussian function due to the instrumental broadening. The binding energy of Pt $4f$ core level of the Pt(111) single crystal was 71.0 eV and the instrumental resolution of 0.9 and 1.3 eV (FWHM) for the pass energies of 100 and 150 eV, respectively.

Auger-electron measurements were taken using a Perkin Elmer AES system equipped with a cylindrical mirror analyzer using 5-keV primary electrons. The signals were measured as the peak-to-peak amplitude of the Pd(330 eV) feature and were normalized with the amplitude of the Pd(330 eV) peak for polycrystalline bulk palladium under the same experimental conditions. LEED measurements were performed using Reverse View LEED equipment from Princeton Applied Research, Inc.

III. RESULTS AND DISCUSSION

Figure 2(a) shows the plot of the Pd(330 eV) Auger-electron intensity versus deposition time. The palladium signal increases linearly with the deposition time until $t=44$ sec, when the first deviation from the linearity is shown. This discontinuity corresponds to completion of the first monolayer of the deposit. As shown in Fig. 2(b), the data may be interpreted using a layer-by-layer growth model with the inelastic mean free path (IMFP) of λ(Pd 330 eV)=8.1 Å. We have assumed here that the growth of the Pd(111) planes occurs with the same density as in the crystal palladium. The IMFP value of the Pd(330 eV) electron, 8.1 Å, agrees well with the calculated values λ(Pd 330 eV)=8.4 (Ref. 35) and 8.0 Å (Ref. 36). In agreement with the layer-by-layer growth model, we have not found fractional LEED spots that would correspond to registries other than those of the (1×1) palladium deposits.

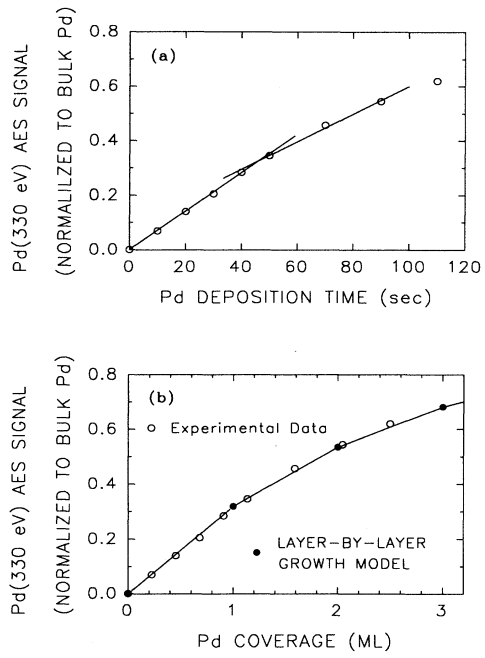

FIG. 2. (a) Plot of Auger-electron intensity, normalized Pd (330 eV) peak-to-peak amplitude, vs palladium deposition time. Solid lines are guides to the eye. (b) Auger-electron intensity of Pd (330 eV) (open dots) and a layer-by-layer growth model line (filled dots and solid line).

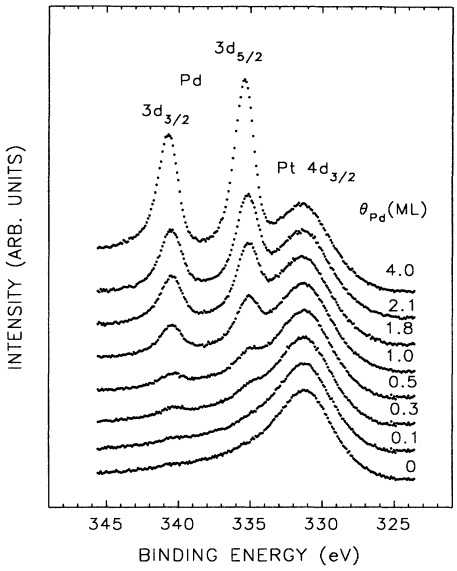

FIG. 3. X-ray photoelectron spectra of the Pd $3d$ and Pt $4d_{3/2}$ core levels for palladium adlayers deposited on Pt(111) with Θ_{Pd}=0, 0.1, 0.3, 0.5, 1.0, 1.8, 2.1, and 4.0 ML.

Figure 3 shows x-ray photoelectron spectra of Pd $3d$ and Pt $4d_{3/2}$ core levels at palladium coverages Θ_{Pd}=0, 0.1, 0.3, 0.5, 1.0, 1.8, 2.1, and 4.0 ML. Pt $4f$ core-level spectra are shown in Fig. 4 for the same coverages. To interpret these data, one should recall that the x-ray pho-

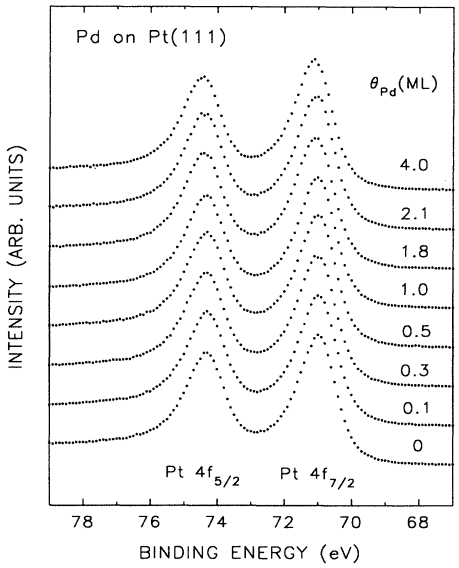

FIG. 4. X-ray photoelectron spectra of Pt $4f$ core levels for palladium adlayers deposited on Pt(111).

toelectron spectra of metals are described by the joint density of states between the initial N-body ground state and the final states of the $(N-1)$ body after the creation of a photoelectron. The common factors governing the line shape and the energy position of the core-level x-ray photoelectron spectra are the photoionization cross section of the core level, the lifetime of the photoexcited core hole, the relaxation energy and screening of the final-state core hole, the energy-loss features created as the photoelectron travels through the solid and excites plasmons, low-energy excitons at around the Fermi level, and shakeup satellites. Influential here also are different chemical states at similar energies due to the inhomogeneity of the sample surface and the difference in the chemical states between the surface and bulk atoms. Finally, the instrumental broadening should be considered including the finite width of the photon source and the phonon broadening at room temperature, as well as the inelastic-scattering background.

Considering the lifetime broadening and creation of low-energy electron-hole pairs (excitons) under the assumption of constant density of states (DOS) at around the Fermi level, Doniach and Šunjic[37] have obtained an expression for the XPS line shape of the form

$$I(E)=\frac{\Gamma(1-\alpha)\cos\left[\frac{1}{2}\pi\alpha+(1-\alpha)\arctan\left[\frac{E}{\gamma}\right]\right]}{(E^2+\gamma^2)^{(1-\alpha)/2}}, \quad (1)$$

where E is the energy from the center position of the peak, Γ the gamma function, 2γ the full width at half maximum (FWHM) of the core-hole Lorentzian line shape, and α the asymmetry parameter (singularity index) due to creation of low-energy excitons at the Fermi sea. This Doniach-Šunjic shape has proven successful for the core levels of many simple metals.[38,39] However, for some metals such as Pd and Pt, Eq. (1) is not fit well since a sharp change of the DOS at around the Fermi level breaks the approximations involved.[23,39,40]

To separate efficiently the contributions from the Pd $3d$ and Pt $4d_{3/2}$ core levels to the x-ray photoelectron spectra in the same energy region, we have obtained a Pt $4d_{3/2}$ line shape using a pure platinum core-level spectrum by convoluting a Doniach-Šunjic function and a Gaussian form due to instrumental broadening, as shown in Fig. 5(a). Here, we set the Gaussian, the Lorentzian, and the asymmetry parameters free to improve the fitness in χ^2-minimization procedure. The fit is good as is demonstrated by the coincidence of the experimental data (dotted line) and the calculated result (solid line), as well as by the residual (dashed line) shown in Fig. 5. To deconvolute the Pd $3d$ spectra overlapping with the Pt $4d_{3/2}$ peak we have used this Pt $4d_{3/2}$ line shape by fixing all its characteristic parameters except the peak height and the energy position.

Figure 5(b) shows an example of the x-ray photoelectron spectrum of Pd $3d$ and Pt $4d_{3/2}$ core levels and its numerical analysis results at $\Theta_{Pd}=1.0$ ML. In the course of the χ^2 fitting procedure the following free parameters were involved: the intensity ratio of Pd $3d_{5/2}$ and Pd $3d_{3/2}$ photoelectron lines together with their binding energies and intensities, the Lorentzian natural linewidth, the asymmetry parameter as characterized in Eq. (1), and the Gaussian (instrumental) broadening. The instrumental broadening was 1.3 ± 0.1 eV (FWHM), comparable with the value obtained from the Fermi edge broadening. The Lorentzian natural linewidths were 0.30 ± 0.15 eV (FWHM) at coverages below 0.4 ML, and 0.5 ± 0.1 eV elsewhere. The theoretical value of 0.35 ± 0.05 eV (Ref. 30) is in accord with the former value, while the latter is somewhat higher. We will discuss this change of the peak width in more detail later. At present, we note that the Pd($3d_{3/2}$)/Pd($d_{5/2}$) intensity ratio of 0.7 is slightly higher than the expected value of $\frac{2}{3}$. One of the reasons for this deviation is the $4d$ electron shakeup process.[23,40] Since the Pd $3d_{3/2}$ electron is more strongly bound than the Pd $3d_{5/2}$ one, another possibility to account for our observation is the Coster-Kronig decay of the $3d_{3/2}$ hole into a $3d_{5/2}$ hole and a simultaneous $4d$ valence-electron excitation (M_4M_5V).[41] The spin-orbit splitting energy between Pd $3d_{5/2}$ and Pd $3d_{3/2}$ varied from 5.30 eV at $\Theta=4.0$ ML to 5.25 eV at the lowest coverage, which is in agreement with the literature values.[23,32] This slight variation may be related to the change of chemical states between full and submonolayer coverage regions on the Pt(111) substrate. The asymmetry parameter α decreases from 0.08 at $\Theta=4.0$ ML to 0.06 at the lowest coverage. This parameter reflects the extent of screening of the core hole by valence-band electrons.[37,42] The decrement of this value indicates that the Pd $4d$ valence band is nar-

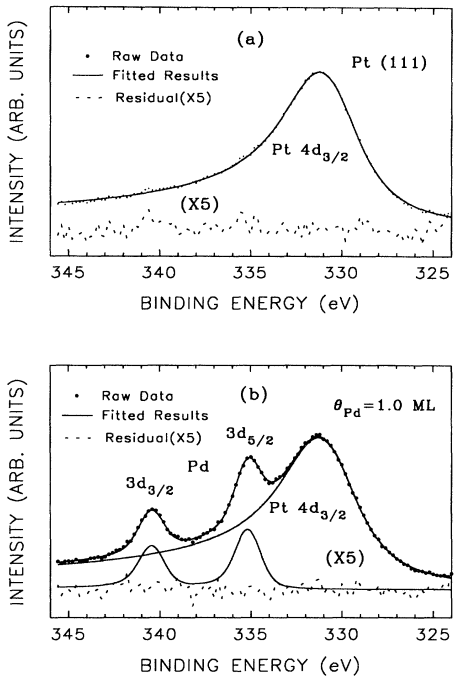

FIG. 5. X-ray photoelectron spectra (dots) of the Pt $4d_{3/2}$ and Pd $3d$ core levels and their fitted curves (solid lines) for (a) a pure Pt(111) and (b) the palladium adlayers deposited on the Pt(111) with $\Theta_{Pd}=1.0$ ML. The residuals (five times) are shown with dashed lines.

rowed and filled, and the DOS at the Fermi level is reduced as the palladium coverage decreases.

It is crucial to determine the change of the core-level binding energy and the peak width at the palladium coverage varies. To do so, we have fixed the asymmetry parameter to an intermediate value of 0.07. Since the change of the asymmetry parameter associated with the peak-position variation is less than 0.03 eV, and the change of peak width below 0.06 eV is negligible, the above simplification may be justified. Figure 6 represents (a) the peak widths and (b) the binding energies of the Pd $3d_{5/2}$ core level. The peak width was determined as the FWHM of the fitted Pd $3d_{5/2}$ spectrum and includes the instrumental broadening as well as the natural line broadening. We allowed deviations of fitting parameters within a 95% confidence limit of the χ^2 value and displayed them as the vertical bars at the data points in Fig. 6. The dashed lines are introduced to guide the eye.

The results give a Pd $3d_{5/2}$ core-level binding energy of 334.9 eV at coverages below 0.4 ML. This increases by 0.2 eV and flattens at higher coverages until about two monolayers of palladium is obtained. At 4.0 ML coverage, the binding energy increases to 335.3 eV. Note that, at coverages below 0.4 ML, the Pd $3d$ core level has apparently a lower binding energy and a smaller peak width. We may ascribe the narrower peak to a single component of the surface adatoms at coverages below 0.4 ML. It is natural that the lifetime of the core level decrease as the cluster size increases due to a faster decay of the core hole in larger size clusters with an efficient screening effect. And also different chemical states of outermost surface and full covered layers might make a core-level line shape broaden. In our case, the core-level width (inversely proportional to the lifetime of photoexcited core hole) jumped up to a higher value at the coverages higher than 0.4 ML as shown in Fig. 6(a). This indicates that adatom clusters may start to agglomerate at this coverage and form a somewhat large dimension of two-dimensional adatom islands even in submonolayer region. The peak widths at higher coverages probably represent a mixed contribution from different chemical states of outermost surface and full covered adatom layers.

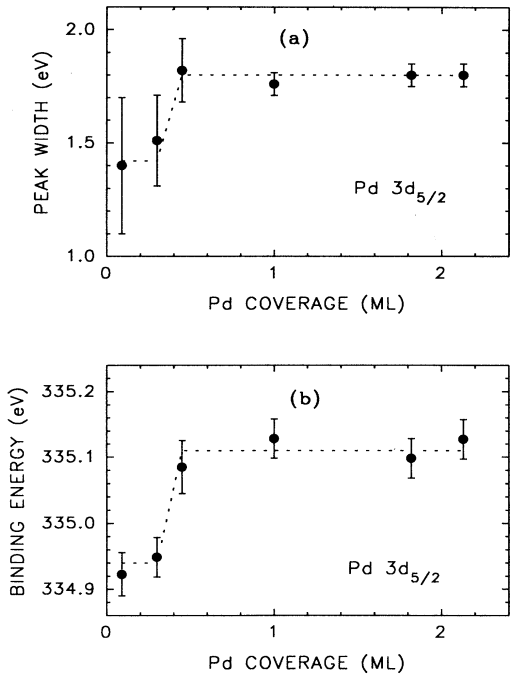

FIG. 6. (a) The full width at half maximum values and (b) binding energies of the Pd $3d_{5/2}$ core level as a function of the coverage for palladium adlayers on Pt(111). The dashed lines are introduced to guide the eye. The error analysis is given in the text.

The electron core-level binding energy in metallic clusters usually increases upon decreasing the coordination number due to a poorly screened final-state effect.[3,18] This was established experimentally for predominantly flat, small palladium clusters on carbon.[17–23] Due to the latter findings, one could expect that during palladium deposition on the Pt(111) substrate, the palladium core-level binding energy should be the highest at the lowest coverage. This would result in a binding-energy decrease with the increase in palladium coverage. Unexpectedly, the results of our study show the opposite trend: the lower the palladium coverage, the lower the Pd $3d$ binding energy [Fig. 6(b)]. This negative binding-energy shift at the low coverages or on the surface compared to the bulk value has been investigated for elemental noble metals and interpreted as purely an initial state origin by Wertheim and Citrin.[25] Wertheim[18] has suggested that the $4d$ valence and $5s$ conduction bands of palladium should narrow and separate from each other with decreasing size of the palladium clusters. As a net result, the intra-atomic charge transfer from the $5s$ band to the $4d$ band should occur to move the system toward the Pd atomic configuration. It is obvious that the exact $4d^{10}5s^0$ configuration of the isolated palladium atom is not attained, even for a few-atom cluster. If the centroid of the valence band was not changed, the narrowing of the almost filled $4d$ band would move the top edge of the valence band away from the vacuum level, and make initially unoccupied states filled. Due to the fact that each atom tends to keep the same number of occupied electronic states per atom for charge neutrality, the centroid of the valence band as well as the surface-atom core levels move towards vacuum level as shown in Fig. 1(a).[25,26] Since the binding energy is determined by the energy distance from the Fermi level, one can expect a negative binding-energy shift at the low coverage, or on the surface atoms compared to the bulk value, due to the purely initial-state origin.[18,25] The negative core-level binding-energy shift of surface palladium atoms on a bulk palladium due to the initial-state origin has recently been confirmed by Nyholm *et al.* for the Pd(100) single-crystal system.[28]

As mentioned in the Introduction, the same core-level binding-energy shifts of the adatom have previously been seen for some other bimetallic systems.[30,33] Somorjai *et al.* noticed that the portion of adatom-cluster edges increases as the gold coverage goes to zero for the Au/Pt(100) system.[33] Since the edge atoms have lower

coordination number and narrower bandwidth, the negative binding-energy shift at the lower coverage was interpreted as the effect of coordination-number change of the top-layer atoms due to the initial-state origin.[25,33] Therefore, the binding-energy shift for the Pd/Pt(111) system with palladium coverage observed by us can be understood in terms of the decrease of the coordination number of the overlayer atoms and the concomitant band narrowing of the overlayer adatom system.

The positive binding-energy shift for many palladium clusters[17–23] and bimetallic systems[29–32] has been explained by the final-state effect. Note that the final-state effect on the other systems is attributed to the poor screening of the core hole after creating the photoelectron. The difference of the Pd $3d_{5/2}$ binding energy between the lowest (0.09 ML) and the highest (4.0 ML) coverages examined in this work is about 0.4 eV. This is close to the surface-atom core-level shift of 0.44 eV for the Pd(100) surface investigated recently.[28] Since the valence-band electrons in elemental metals usually are strongly hybridized by themselves, the final-state core hole in these materials is efficiently screened. As a result, no final-state effect is expected in the XPS core levels of elemental metals. Since the Pd/Pt(111) system shows also no final-state effect after creating a core hole, the efficient screening or very fast relaxation may occur in this system. This is strikingly different from the other palladium bimetallic systems[29–32] and palladium clusters[17–23] in which the final-state effect may compensate for the initial-state contribution to the core-level shift. Therefore, the absence of the final-state effect in the Pd/Pt(111) system indicates that hybridization of the valence bands of the palladium adlayer and the platinum substrate plays an important role in the negative surface-atom binding-energy shift of the Pd 3*d* core level.

IV. CONCLUSIONS

The results of the AES analysis are well fit by a layer-by-layer growth model, and yield an inelastic mean free path (IMFP) of λ(Pd 330 eV)=8.1 Å. This is in good agreement with the calculated values of λ=8.4 and 8.0 Å. The LEED patterns showed no other than the (1×1) structure of palladium adatoms on Pt(111) in the studied coverage range (<4 ML), supporting the Frank–van der Merve growth mechanism.

In contrast to many palladium clusters and palladium bimetallic systems, the 3*d* core-level binding energy of palladium deposited on Pt(111) substrate shifts with decreasing palladium coverage (or the coordination number) toward the lower binding energy. This shift results mainly from the initial-state band-narrowing effect predicted by Citrin, Wertheim, and Baer, and can be understood in terms of the coordination number change and the concomitant band narrowing of the overlayer adatoms.

The Pd 3*d* core level has a lower binding energy and a narrower peak width at coverages below 0.4 ML. We ascribe the narrower peak to the single component of the surface adatoms at coverages below 0.4 ML. Adatom clusters may start to agglomerate at this submonolayer coverage and form a somewhat large dimension of two-dimensional adatom islands. The peak widths at higher coverages represented a mixed contribution from different chemical states of outermost surface and full covered adatom layers.

ACKNOWLEDGMENTS

We appreciate numerous and valuable discussions with Dr. H. H. Farrell. This work was supported by National Science Foundation Grant No. DMR-89-20538, through the Materials Research Laboratory of the University of Illinois. M.H. acknowledges support by Air Force Office of Scientific Research Grant No. AFOSR-89-0368. We acknowledge use of the facilities in the Center for Microanalysis of Materials at the University of Illinois, which is supported by the U.S. Department of Energy under Contract No. DEFG02-91-ER45439.

[1] C. Argile and G. E. Rhead, Surf. Sci. Rep. **10**, 277 (1989).
[2] J. A. Rodriguez and D. W. Goodman, Surf. Sci. Rep. **14**, 1 (1991).
[3] W. F. Egelhoff, Surf. Sci. Rep. **6**, 253 (1987).
[4] Z. Karpinski, Adv. Catal. **37**, 45 (1990).
[5] M. W. Ruckman and M. Strongin, Phys. Rev. B **29**, 7105 (1984).
[6] S. Xinyin, D. J. Frankel, J. C. Hermanson, G. J. Lapeyre, and R. J. Smith, Phys. Rev. B **32**, 2120 (1985).
[7] X. Y. Shen, D. J. Frankel, G. J. Lapeyre, and R. J. Smith, Phys. Rev. B **33**, 5372 (1986).
[8] B. Frick and K. Jacobi, Phys. Rev. B **37**, 4408 (1988).
[9] B. E. Koel, R. J. Smith, and P. J. Berlowitz, Surf. Sci. **231**, 325 (1990).
[10] B. E. Koel, A. Selldj, and M. T. Paffett, Phys. Rev. B **46**, 7846 (1992).
[11] G. A. Attard and A. Bannister, J. Electroanal. Chem. **300**, 467 (1991).
[12] J. Clavilier, M. J. Lorca, J. M. Feliu, and A. Aldaz, J. Electroanal. Chem. **310**, 429 (1991).
[13] G. L. Kellog, Phys. Rev. B **45**, 14 354 (1992).
[14] G. N. Burland and P. J. Dobson, Thin Solid Films **74**, 383 (1981).
[15] G. C. Smith, C. Norris, C. Binns, and H. A. Padmore, J. Phys. C **15**, 6481 (1982).
[16] F. J. Kuijers, B. M. Tieman, and V. Ponec, Surf. Sci. **75**, 657 (1978).
[17] Ch. Kuhrt and M. Harsdorff, Surf. Sci. **245**, 173 (1991).
[18] G. K. Wertheim, Z. Phys. D **12**, 319 (1989).
[19] G. K. Wertheim and S. B. DiCenzo, Phys. Rev. B **37**, 844 (1988).
[20] G. K. Wertheim, S. B. DiCenzo, and D. N. E. Buchanan, Phys. Rev. B **33**, 5384 (1986).
[21] S. Kohiki and S. Ikeda, Phys. Rev. B **34**, 3786 (1986).
[22] A. Fritsch and P. Légaré, Surf. Sci. **162**, 742 (1985).
[23] T. T. P. Cheung, Surf. Sci. **140**, 151 (1984); **127**, L129 (1983).
[24] M. Cini, M. DeCrescenzi, F. Patella, N. Motta, M. Sastry, F. Rochet, R. Pasquali, and A. Balzarotti, Phys. Rev. B **41**, 5685 (1990).
[25] P. H. Citrin, G. K. Wertheim, and Y. Baer, Phys. Rev. Lett.

41, 1425 (1978).
[26]M. C. Desjonquères, D. Spanjaard, Y. Lassailly, and C. Guillot, Solid State Commun. **34**, 807 (1980).
[27]P. H. Citrin, G. K. Wertheim, and Y. Baer, Phys. Rev. B **27**, 3160 (1983).
[28]R. Nyholm, M. Qvarford, J. N. Andersen, S. L. Sorensen, and C. Wigren, J. Phys. Condens. Matter **4**, 277 (1992).
[29]G. W. Graham, P. J. Schmitz, and P. A. Thiel, Phys. Rev. B **41**, 3353 (1990).
[30]J. A. Rodriguez, R. A. Campbell, and D. W. Goodman, J. Phys. Chem. **94**, 6936 (1990).
[31]V. S. Sundaram, M. B. de Moraes, J. G. Rogers, and G. G. Kleiman, J. Phys. F **11**, 1151 (1981).
[32]F. U. Hillebrecht, J. G. Fuggle, P. A. Bennett, and Z. Zolnierek, Phys. Rev. B **27**, 2179 (1983).
[33]M. Salméron, S. Ferrer, M. Jazzar, and G. A. Somorjai, Phys. Rev. B **28**, 1158 (1983).
[34]P. Zelenay and A. Wieckowski, J. Electrochem. Soc. **139**, 2552 (1992); P. Zelenay, L. M. Rice-Jackson, A. Wieckowski, and J. Gawlowski, Surf. Sci. **256**, 253 (1991).
[35]S. Tanuma, C. J. Powell, and D. R. Penn, Surf. Interface Anal. **17**, 911 (1991).
[36]M. P. Seah and W. A. Dench, Surf. Interface Anal. **1**, 2 (1979).
[37]S. Doniach and M. Šunjic, J. Phys. C **3**, 285 (1970).
[38]P. H. Citrin, G. K. Wertheim, and Y. Baer, Phys. Rev. B **16**, 4256 (1977).
[39]G. K. Wertheim and P. H. Citrin, in *Photoemission in Solids I,* edited by M. Cardona and L. Ley (Springer, Berlin, 1978), p. 197.
[40]S. Hüfner and G. K. Wertheim, Phys. Rev. B **11**, 678 (1975).
[41]N. Mårtensson, R. Nyholm, and B. Johansson, Phys. Rev. Lett. **45**, 754 (1980).
[42]G. D. Mahan, Phys. Rev. **163**, 612 (1967); P. Nozières and C. T. DeDominicis, *ibid.* **178**, 1097 (1969).